Eur. Phys. J. B **55**, 283–288 (2007)
DOI: 10.1140/epjb/e2007-00055-1

THE EUROPEAN PHYSICAL JOURNAL B

# Linear and nonlinear intersubband optical absorptions in an asymmetric rectangular quantum well

İ. Karabulut[1,a], Ü. Atav[1], H. Şafak[1], and M. Tomak[2]

[1] Department of Physics, Selçuk University, Konya 42075, Turkey
[2] Department of Physics, Middle East Technical University, Ankara 06531, Turkey

Received 16 August 2006 / Received in final form 24 January 2007
Published online 21 February 2007 – 

**Abstract.** The linear and nonlinear intersubband optical absorptions in $Al_{xl}Ga_{1-xl}As/GaAs/Al_{xr}Ga_{1-xr}As$ asymmetric rectangular quantum well are studied within the framework of the density matrix formalism. We have calculated the electron energy levels and the envelope wave functions using the effective mass approach. In addition, we have obtained an expression for saturation intensity. It is shown that the parameters such as asymmetry and width of potential well not only shift the peak positions in absorption spectrum but also considerably modify their height. These results suggest that the absorption process can be easily controlled by the structure parameters of an asymmetric rectangular quantum well. Also, the incident optical intensity has a great effect on the total absorption spectrum. We have seen that the absorption peak is reduced by half when the optical intensity is approximately 0.8 MW/cm$^2$ for well width $L = 90$ Å and $\beta = 0.5$. Moreover, it is seen that the saturation intensity is quite sensitive to the structure parameters of an asymmetric rectangular quantum well. Thus, the results presented here can be useful for electro-optical modulators and photodetectors in the infrared region.

**PACS.** 42.65.Ky Frequency conversion; harmonic generation, including higher-order harmonic generation – 78.67.De Quantum wells

## 1 Introduction

Semiconductor quantum well (QW) structures have attracted a great deal of attention because of their novel electronic and optical properties over the past two decades [1–21]. Quantum confinement of carriers in the semiconductor QW's, which leads to the quantization of energy levels and the formation of subbands, has been studied extensively [1]. These energy levels can be tailored by changing the barrier widths and heights, well widths, and by modifying the shape of a well with different composition profiles and external applied electric fields.

Experimental results have been reported for intersubband optical transitions in a GaAs quantum well [2]. A very large dipole strength along with a narrow bandwith were observed on the absorption spectra. This suggests that intersubband optical transitions in a quantum well may have very large optical nonlinearities. There are many studies associated with both the intersubband optical transitions [3–10] and the nonlinear optical properties induced by interband and intersubband transitions [11–17] in semiconductor quantum wells. Both linear and nonlinear intersubband optical absorptions can be used for practical applications in photodetectors and high-speed electrooptical devices [18,19].

The nonlinear optical properties of semiconductor quantum well mainly depend on the asymmetry of the confining potential. Such an asymmetry in potential profile can be obtained either by applying an electric field to a symmetric quantum well or by compositionally grading the QW. In this paper, a compositionally asymmetric rectangular quantum well (ARQW) of the type $Al_{xl}Ga_{1-xl}As/GaAs/Al_{xr}Ga_{1-xr}As$ is considered. This QW structure has a tunable degree of asymmetry. The tunable asymmetry of the potential is expected to yield promising nonlinear optical properties. Therefore it would be interesting to study the linear and nonlinear optical properties in an ARQW. To the best of our knowledge, this is the first study of the nonlinear optical properties in an ARQW.

In this work, we present only theoretical calculations for the linear and nonlinear optical absorptions associated with intersubband transitions in ARQW. The electronic states in an ARQW are calculated using the effective mass

[a] e-mail: ikarabulut@selcuk.edu.tr

approach. The expressions for the linear and nonlinear intersubband optical absorption coefficients are given within the framework of the density matrix formalism by following references [4,9,17]. The saturation intensity expression is also derived using the same formalism. The dependencies of both the absorption coefficients and the saturation intensity on structure parameters of ARQW are investigated. In particular, the effects of asymmetry and well width are considered. Our results show that both the intersubband absorption spectrum and the saturation intensity depend sensitively on the structure parameters such as the width and asymmetry of the potential well. Moreover, the incident optical intensity has a great effect on the total absorption.

The organization of this paper is as follows: in Section 2, we outline the theory of electronic states and optical absorption calculations in an ARQW. In Section 3, we present and discuss numerical results. A brief conclusion is given in Section 4.

## 2 Theory

We consider ARQW composed of three different semiconductor layers, which are located at $z < -L/2$ (layer $l$), $-L/2 \leqslant z \leqslant L/2$ (layer $w$) and $z > L/2$ (layer $r$).

To calculate the linear and nonlinear intersubband optical absorption coefficients, we need only to consider the dipole matrix elements and energies of the envelope wave functions [17]. The energy levels $E_n$ and the corresponding envelope wave functions $\phi_n(z)$ in a QW may be found by solving Schrödinger equation in the effective mass approach:

$$-\frac{\hbar^2}{2}\frac{d}{dz}\left(\frac{1}{m^*}\frac{d\phi_n(z)}{dz}\right)+V(z)\phi_n(z)=E_n\phi_n(z), \quad (1)$$

where

$$V(z)=\begin{cases} V_l, & z<-L/2 \\ 0, & -L/2\leqslant z\leqslant L/2 \\ V_r, & z>L/2. \end{cases} \quad (2)$$

Here $z$ represents the growth direction, the indices "$l$" and "$r$" indicate that the corresponding parameter belongs to the left and right barrier materials, respectively. $m^*$ is the effective mass depending on the material composition. We assume GaAs to be the quantum well material and $Al_{xi}Ga_{1-xi}As$ ($i = l$, $r$) to be the barrier materials, so that the asymmetric potential is generated by three layers with different Al mole fractions,

$$x(z)=\begin{cases} x_l, & z<-L/2 \\ 0, & -L/2\leqslant z\leqslant L/2 \\ x_r, & z>L/2. \end{cases} \quad (3)$$

The asymmetric potential $V(z)$ is governed by three parameters: $x_l$, $x_r$ and $L$. The parameters $x_l$ and $x_r$ tune the degree of the asymmetry, and the potential profile is symmetric for $x_l = x_r$.

Equation (1) can be solved exactly in each layer (well and barriers) by using the continuity of $\phi_n(z)$ and $1/m^* d\phi_n(z)/dz$ at each boundary [21]. The envelope wave function solution of the Schrödinger equation is then given by

$$\phi_n(z)=N_n\cdot\begin{cases} \sin\theta_l\sin\left(\frac{q_nL}{2}+\theta_r\right)e^{p_{\ln}(z+L/2)}, \\ \quad z<-L/2 \\ \sin\left(\frac{q_nL}{2}+\theta_r\right)\sin\left[q_n\left(z+\frac{L}{2}\right)+\theta_l\right], \\ \quad -L/2\leqslant z\leqslant L/2 \\ \sin\theta_r\sin\left(\frac{q_nL}{2}+\theta_l\right)e^{-p_{rn}(z-L/2)}, \\ \quad z>L/2. \end{cases} \quad (4)$$

Further, we derive the following relation to determine the electron subband energies $E_n$,

$$tg(q_nL)=\frac{q_nm_w\left(m_lp_{rn}+m_rp_{\ln}\right)}{q_n^2m_lm_r-p_{\ln}p_{rn}m_w^2}. \quad (5)$$

Here $\theta_i$ is defined as

$$\theta_i=\arcsin\frac{1}{\sqrt{1+\frac{p_{in}^2m_w^2}{q_n^2m_i^2}}}, \quad (i=r,l) \quad (6)$$

where $p_{in}=\sqrt{2m_i(V_i-E_n)}/\hbar$ , $q_n=\sqrt{2m_wE_n}/\hbar$ and $N_n$ is the normalization constant.

The susceptibility $\chi$ is related to the absorption coefficient $\alpha(\omega)$ by

$$\alpha(\omega)=\omega\sqrt{\frac{\mu}{\varepsilon_R}}\mathrm{Im}\left[\varepsilon_0\chi(\omega)\right], \quad (7)$$

where $\mu$ is the permeability of the system, $\varepsilon_R$ is the real part of the permittivity. Using the density matrix method analogous to those of references [4,9], the linear and third order nonlinear optical absorption coefficients in an ARQW can be derived as follows:

$$\alpha^{(1)}(\omega)=\omega\sqrt{\frac{\mu}{\varepsilon_R}}\frac{|M_{21}|^2\sigma_s\hbar\Gamma_0}{(E_2-E_1-\hbar\omega)^2+(\hbar\Gamma_0)^2}, \quad (8)$$

$$\alpha^{(3)}(\omega,I)=-2\omega\sqrt{\frac{\mu}{\varepsilon_R}}\left(\frac{I}{\varepsilon_0n_Rc}\right) \times\frac{|M_{21}|^4\sigma_s\hbar\Gamma_0}{\left[(E_2-E_1-\hbar\omega)^2+(\hbar\Gamma_0)^2\right]^2}\left(1-\frac{|M_{22}-M_{11}|^2}{|2M_{21}|^2} \times\frac{\left\{(E_2-E_1-\hbar\omega)^2-(\hbar\Gamma_0)^2+2(E_2-E_1)\left(E_2-E_1-\hbar\omega\right)\right\}}{(E_2-E_1)^2+(\hbar\Gamma_0)^2}\right), \quad (9)$$

where $\sigma_s$ is the electron density, $E_1(E_2)$ is the initial (final) state energy, $\Gamma_0 = 1/\tau$ is the relaxation rate for states 1 and 2, $I$ is the incident optical intensity, $n_R$ is the refractive index, $c$ is the speed of light in vacuum and $M_{ij} = \langle\phi_i|qz|\phi_j\rangle$ is the matrix element ($i$, $j = 1$, 2).

Then the total absorption coefficient is

$$\alpha(\omega,I)=\alpha^{(1)}(\omega)+\alpha^{(3)}(\omega,I). \quad (10)$$

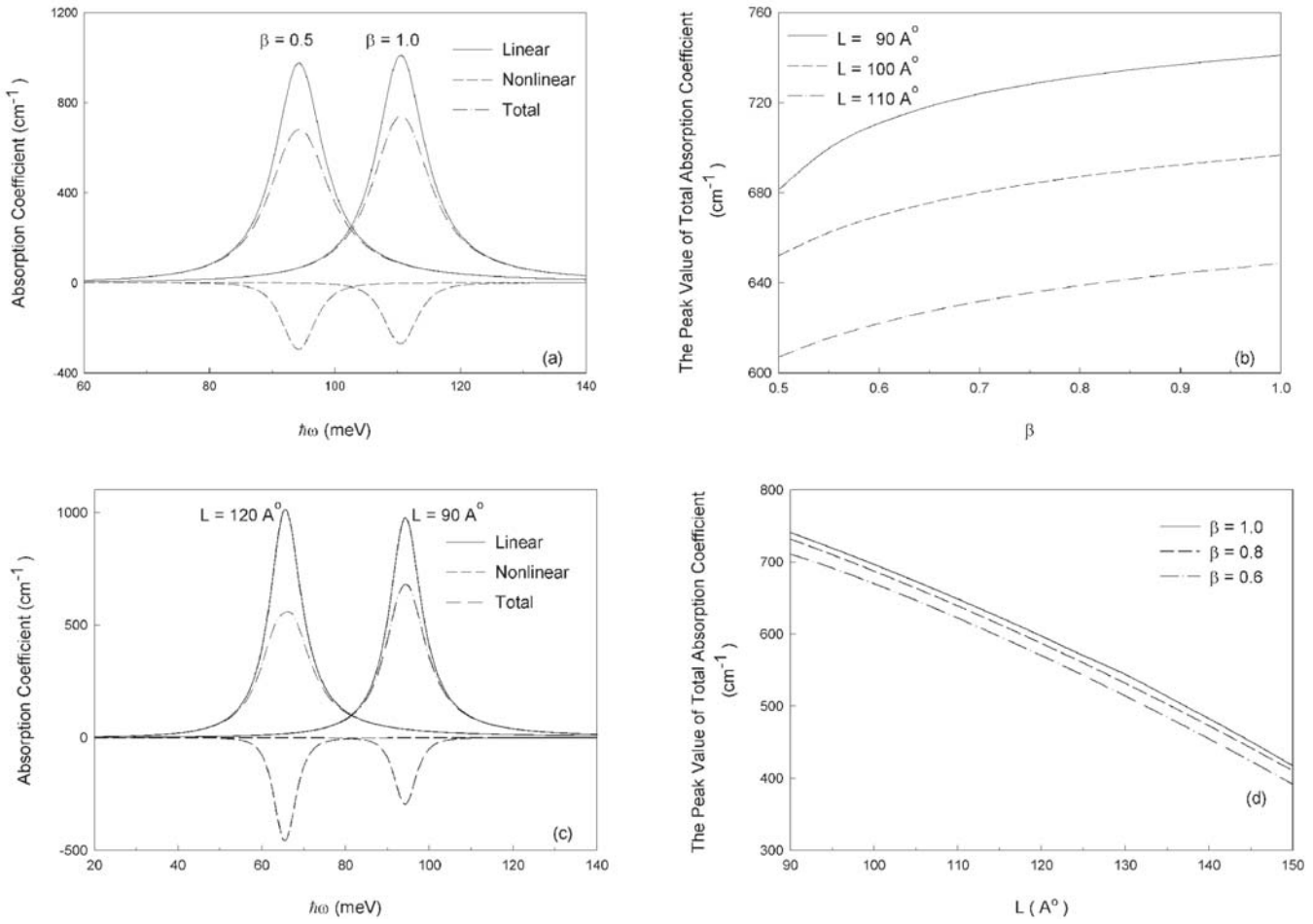


**Fig. 1.** (a) The linear, the nonlinear, and the total absorption coefficients as a function of photon energy for two different $\beta$ values, $I = 0.5$ MW/cm$^2$ and $L = 90$ Å. (b) The resonant peak value of the total absorption coefficient as a function of the parameter $\beta$ for three different $L$ values and $I = 0.5$ MW/cm$^2$. (c) The linear, the nonlinear, and the total absorption coefficients as a function of photon energy for two different $L$ values, $I = 0.5$ MW/cm$^2$ and $\beta = 0.5$. (d) The resonant peak value of the total absorption coefficient as a function of the well width $L$ for three different $\beta$ values and $I = 0.5$ MW/cm$^2$.

## 3 Numerical results and discussions

In this study, $Al_{xl}Ga_{1-xl}As/GaAs/Al_{xr}Ga_{1-xr}As$ quantum well with different stoichiometric ratios $x_l$ and $x_r$ was considered and all calculations were performed using the following parameters: $\sigma_s = 3 \times 10^{16}$ cm$^{-3}$, $\Gamma_0 = 1/0.14$ ps$^{-1}$, $n_R = 3.2$, $x_l = 0.4$. The values of the effective mass [22] and confining potential [23] used in these calculations are given as a function of the stoichiometric ratio as follows: $m = m_0(0.0665 + 0.0835x), V = 600 \times (1.155x + 0.37x^2)$ meV. Also, we define an asymmetry parameter $\beta = x_r/x_l$.

In Figures 1a–1d, the effects of structure parameters such as $\beta$ and well width $L$ on the absorption coefficients are plotted. Figure 1a shows the linear $\alpha^{(1)}(\omega)$, nonlinear $\alpha^{(3)}\omega$, I) and total $\alpha(\omega, I)$ absorption coefficients as a function of the photon energy for two different values of $\beta$, $I = 0.5$ MW/cm$^2$ and $L = 90$ Å. As can be seen from this figure, the large linear contribution due to the $\chi^{(1)}$ term is opposite in sign of the nonlinear contribution due to the $\chi^{(3)}$ term. So the total absorption coefficient $\alpha(\omega, I)$ is significantly reduced by the $\alpha^{(3)}(\omega, I)$ contribution. Therefore, we can say that the contributions of both the linear and the nonlinear absorption coefficients should be considered in the calculation of absorption spectrum of the systems operating especially with a high optical intensity. Also, it is clearly seen from figure that the linear absorption coefficient increases slightly with $\beta$, but the nonlinear term is almost constant. This increase of the linear absorption coefficient leads to the increase of the total absorption coefficient. In order to show the effect of $\beta$ on the total absorption coefficient in an ARQW more clearly, in Figure 1b, we plot the variation of the peak value of the total absorption coefficient as a function of $\beta$ for $I = 0.5$ MW/cm$^2$, $L = 90$, 100 and 110 Å. It can be easily seen form this figure that the total absorption peak increases in magnitude with increasing values of $\beta$. From Figure 1a, it is also seen that the intersubband absorption spectrum shows a blue shift as $\beta$ increases. This shift is due to the increase in the energy

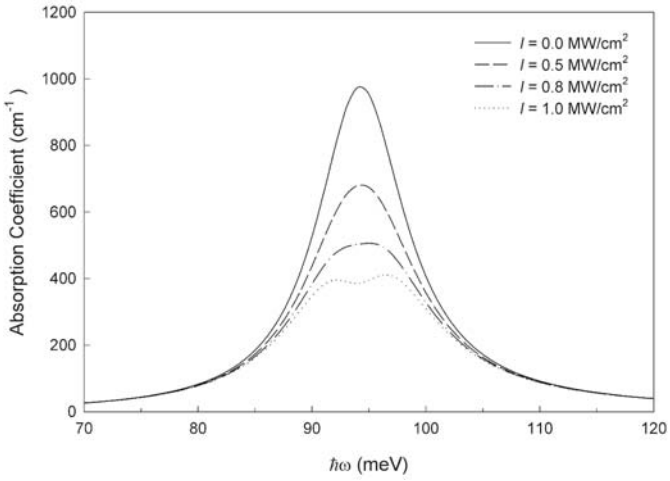


**Fig. 2.** The total absorption coefficient as a function of photon energy for four different $I$ values. $\beta = 0.5$ and $L = 90$ Å.

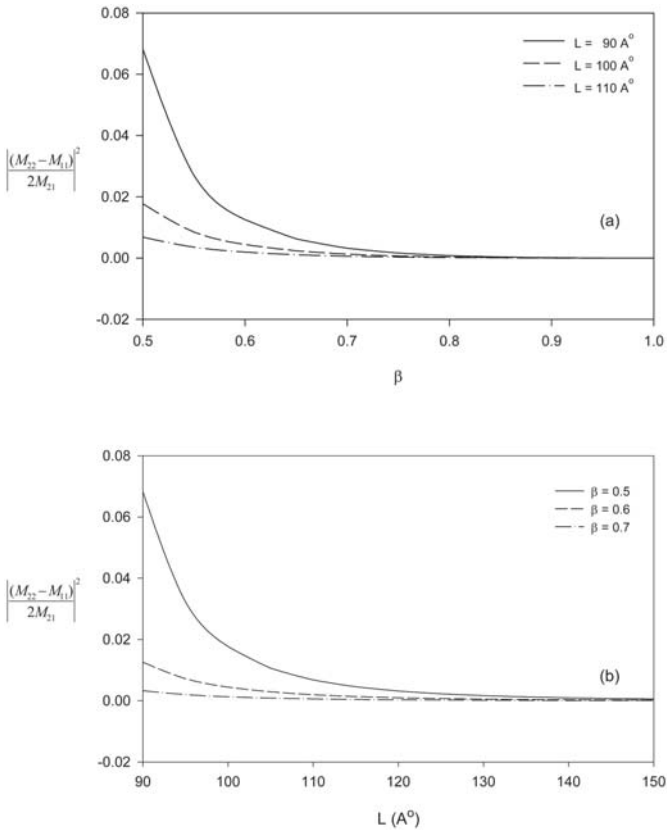


**Fig. 3.** (a) $|(M_{22} - M_{11})/2M_{21}|^2$ is plotted as a function of the $\beta$ for three different $L$ values. (b) $|(M_{22} - M_{11})/2M_{21}|^2$ is plotted as a function of the well width $L$ for three different $\beta$ values.

difference $E_2 - E_1$ between the ground and first excited states with increasing $\beta$ values. The linear, nonlinear and total absorption coefficients are displayed for two different well widths, $I = 0.5$ MW/cm$^2$ and $\beta = 0.5$ as a function of the photon energy in Figure 1c. We see that the peak values of the linear and nonlinear absorption coefficients increase with increasing well width. But, the increase in the nonlinear absorption coefficient is larger than that of linear absorption coefficient. So the variation of the peak value of total absorption spectrum with well width is dominated by the nonlinear absorption term. Therefore, the total absorption peak decreases with increasing well width. It should be noted here that the increasing of well width causes to the weaker confinement of carriers in an ARQW. This weaker confinement, in turn, results in the red shift of absorption spectrum. In Figure 1d, it is interesting that a saturation case is observed on the absorption spectrum for larger well widths. While the peak value of the absorption spectrum is approximately 761 cm$^{-1}$ for $L = 90$ Å and $\beta = 1.0$, this value decreases to 418 cm$^{-1}$ for $L = 150$ Å and same $\beta$ value.

From the discussions given above, it is obvious that both the peak position and the peak magnitude of absorption spectrum in ARQW increase monotonically with $\beta$ but they decrease with $L$. Therefore, in order to obtain a considerable absorption coefficient, we should use an ARQW with the larger $\beta$ and the smaller well width $L$. Such a dependence of absorption spectrum on the structure parameters gives a new degree of freedom in device applications.

Figure 2 shows the total absorption coefficient as a function of the photon energy for four different values of optical intensity $I = 0.0$, 0.5, 0.8 and 1.0 MW/cm$^2$, $\beta = 0.5$ and $L = 90$ Å. The total absorption peak changes considerably with increasing optical intensity. So we can say that one should take into account the nonlinear (intensity-dependent) absorption coefficient near the resonance frequency ($E_{21} \cong \hbar\omega$), especially at higher intensity values. It is well-known that a saturation case is observed on the absorption spectrum of the QW's when the intensity reaches a certain value. We also see that this strong absorption saturation begins to appear at about $I = 0.8$ MW/cm$^2$. The saturation intensity is a characteristic property of QW's and so it would be very useful to investigate this quantity as a function of the structure parameters.

In order to clarify the importance of the saturation intensity, in Figures 3a and 3b, the variations of the square of the ratio of matrix elements $|(M_{22} - M_{11})/2M_{21}|^2$ are plotted against $\beta$ and $L$ respectively. It is clearly seen from these figures that $|(M_{22} - M_{11})/2M_{21}|^2$ term becomes too small compared to unity. We can neglect safely the second term of equation (9) because both the $|(M_{22} - M_{11})/2M_{21}|^2$ term and the other factor in the last term of equation (9) are much smaller than unity. Then, the total absorption coefficient can be given as follows:

$$\alpha(\omega, I) = \alpha^{(1)}(\omega)\left[1 - \left(\frac{2I}{\varepsilon_0 n_R c}\right)\frac{|M_{21}|^2}{(E_2 - E_1 - \hbar\omega)^2 + (\hbar\Gamma_0)^2}\right]. \quad (11)$$

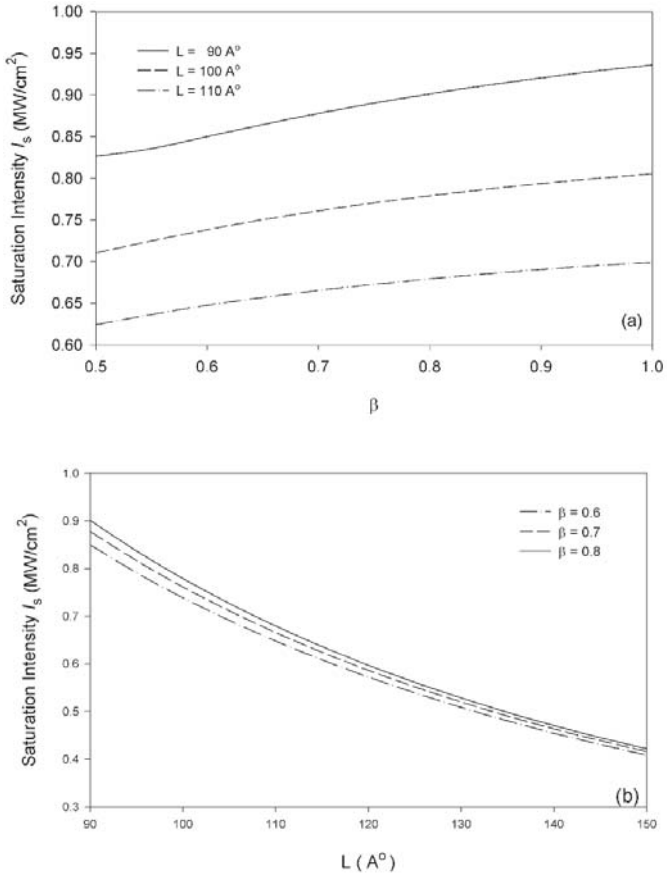


**Fig. 4.** (a) The saturation intensity is plotted as a function of the $\beta$ for three different L values. (b) The saturation intensity is plotted as a function of the L for three different $\beta$ values.

The so-called saturation intensity $I_s$ is defined as the intensity at which the total absorption coefficient $\alpha(\omega, I)$ is reduced by one-half, then we have the relation $\alpha(\omega, I_s) = \alpha^{(1)}(\omega)/2$ or equivalently $\alpha^{(3)}(\omega, I_s) = -\alpha^{(1)}(\omega)/2$. Considering these relations, the saturation intensity can be defined as

$$I_s = \varepsilon_0 n_R c \left( \frac{(E_2 - E_1 - \hbar\omega)^2 + (\hbar\Gamma_0)^2}{|2M_{21}|^2} \right). \qquad (12)$$

Figures 4a and 4b show the saturation intensity as a function of $\beta$ and $L$ respectively. As can be seen also from equation (12), the saturation intensity is inversely proportional to the square of the matrix element $M_{21}$. Therefore, the dependence of saturation intensity on the structure parameters is governed mainly by $|M_{21}|^2$. These two figures show that the saturation intensity increases with $\beta$, but it decreases with increasing well width. It should be noted from Figure 4b that the saturation intensity reaches a certain value with increasing well width. This value is nearly 0.4 MW/cm$^2$ for all $\beta$ values. So we can conclude that the drop of the absorption coefficient will not be very significant when an optical intensity below this value is used. Such a dependence of saturation intensity on the structure parameters in an ARQW can be very useful for several potential device applications.

## 4 Conclusions

We have theoretically calculated the linear and nonlinear intersubband optical absorption coefficients in an ARQW. The energy levels and the corresponding wave functions in an ARQW are obtained within the framework of effective mass approximation. The effective mass mismatch between the well and barrier materials is taken into account in our calculations. The explicit expressions for the linear and nonlinear absorption coefficients are given using the density matrix formalism. Numerical calculations are performed for $Al_{xl}Ga_{1-xl}As/GaAs/Al_{xr}Ga_{1-xr}As$ quantum well with different stoichiometric ratios $x_l$ and $x_r$. Firstly, we have considered the effects of structure parameters such as $\beta$ and $L$ on the absorption coefficients. The results obtained show that the peak value and position of the total absorption spectrum can be considerably modified and controlled by the structure parameters. Also, we see from our calculations that we should use an ARQW with the larger $\beta$ and the smaller well width $L$, in order to obtain a large absorption coefficient. The sensitivity to the structure parameters of the absorption coefficients can be used in various device applications based on the intersubband transitions. We have also observed that a saturation occurs on the absorption spectrum for larger well widths. In addition, the effect of incident optical intensity on the total absorption spectrum is considered. We see that the total absorption peak changes considerably with optical intensity. So the nonlinear (intensity-dependent) absorption coefficient near the resonance frequency ($E_{21} \cong \hbar\omega$), especially at higher intensity values should not be neglected. Our calculations show that the peak value of the total absorption coefficient is reduced by half when the intensity is approximately 0.8 MW/cm$^2$ for the well width, $L = 90$ Å and $\beta = 0.5$. Moreover, we have obtained an expression for the saturation intensity. The variation of this quantity with the structure parameters is investigated. It is seen that the saturation intensity can also be controlled by the structure parameters. This behavior of the saturation intensity can be used in various optical device applications such as far infrared laser amplifiers, photo-detectors, and high-speed electro-optical modulators.

This work is partially supported by the BAP office of Selcuk University.

## References

1. M.J. Kelly, *Low Dimensional Semiconductors* (Oxford, UK, Oxford, 1995)
2. L.C. West, J.J. Eglash, Appl. Phys. Lett. **46**, 1156 (1985)
3. D. Ahn, S.L. Chuang, Phys. Rev. B **35**, 4149 (1987)
4. D. Ahn, S.L. Chuang, IEEE J. Quantum Electron. **QE-23**, 2169 (1987)

5. C. Sirtori, F. Capasso, D.L. Sivco, A.Y. Cho, Phys. Rev. Lett. **68**, 1010 (1992)
6. C. Sirtori, F. Capasso, J. Faist, S. Scandolo, Phys. Rev. B **50**, 8663 (1994)
7. J. Li, C.Z. Ning, Phys. Rev. B **70**, 125309 (2004)
8. P.F. Yuh, K.L. Wang, J. Appl. Phys. **65**, 4377 (1989)
9. E.M. Goldys, J.J. Shi, Phys. Stat. Sol. B **210**, 237 (1998)
10. M. Bedoya, A.S. Camacho, Phys. Rev. B **72**, 155318 (2005)
11. M.K. Gurnick, T.A. DeTemple, IEEE J. Quantum Electron. **QE-19**, 791 (1983)
12. G. Almogy, A. Yariv, J. Nonlin. Opt. Phys. **4**, 401 (1995)
13. J.B. Khurgin, Semicond. Semimetals **59**, 1 (1999)
14. E. Rosencher, Ph. Bois, Phys. Rev. B **14**, 11315 (1991)
15. İ. Karabulut, H. Şafak, M. Tomak, Solid State Commun. **135**, 735 (2005)
16. İ. Karabulut, H. Şafak, Physica B **368**, 82 (2005)
17. H. Yıldırım, M. Tomak, Eur. Phys. J. B **50**, 559 (2006)
18. F. Caposso, K. Mohammed, A.Y. Cho, IEEE J. Quantum Electron. QE-22, 1853 (1986)
19. D.A.B. Miller, Int. J. High Speed Electron. Syst. **1**, 19 (1991)
20. H. Schneider, F. Fuchs, B. Dischler, J. D. Ralston, P. Koidl, Appl. Phys. Lett. **58**, 2234 (1991)
21. G. Bastard, Phys. Rev. B **24**, 5693 (1981)
22. S. Adachi, J. Appl. Phys. **58**, R1 (1985)
23. H.J. Lee, L.Y. Juravel, J.C. Woolley, A.J.S. Thorpe, Phys. Rev. B **21**, 659 (1980)
24. R.W. Boyd, *Nonlinear Optics* (Academic Press, San Diego, 2003)
25. N. Bloembergen, *Nonlinear Optics* (World Scientific, Singapore, 1996)